

Ultra high molecular weight polyethylene with improved plasticity and toughness by high temperature melting

Jun Fu^{a,b}, Bassem W. Ghali^a, Andrew J. Lozynsky^a, Ebru Oral^{a,b,*}, Orhun K. Muratoglu^{a,b}

^a Harris Orthopaedic Laboratory, Massachusetts General Hospital, Boston, MA 02114, United States

^b Department of Orthopedic Surgery, Harvard Medical School, Boston, MA, United States

ARTICLE INFO

Article history:

Received 19 January 2010

Received in revised form

30 March 2010

Accepted 3 April 2010

Available online 14 April 2010

Keywords:

High temperature melting

Wear

Total joint implants

ABSTRACT

Our goal was to improve the strength and toughness of ultra high molecular weight polyethylene (UHMWPE), which is the preferred polymeric bearing material in total joint implants. Based on accelerated diffusion of UHMWPE chains at high temperatures, our hypothesis was that high temperature melting could minimize the structural defects and thus improve the toughness of consolidated UHMWPE. Melting of consolidated medical-grade UHMWPE at 280, 300, and 320 °C in inert atmosphere improved the elongation at break, work-to-failure and impact strength, presumably due to chain scissioning and structural defect elimination through self-diffusion. An important finding of this study was that the gain in plasticity and toughness did not sacrifice the wear resistance under optimized melting conditions, which may be promising for next generation high performance UHMWPE materials for joint implant bearing surfaces.

© 2010 Elsevier Ltd. All rights reserved.

1. Introduction

Ultra high molecular weight polyethylene (UHMWPE) has been the material of choice for total joint implants for over four decades. The longevity of UHMWPE implants has been limited by its wear and oxidation resistance, especially after radiation sterilization [1,2]. While high dose radiation cross-linking has decreased wear [3] together with the use of antioxidant stabilization to minimize oxidation [4], it has also decreased the mechanical strength of joint implants, limiting its use in high stress applications such as total knee implants, especially in younger and more active patients. Thus, there is an increasing desire to improve the strength and toughness of radiation crosslinked UHMWPEs. In this paper, we present a method by which the toughness of the consolidated UHMWPE is increased for further treatment with cross-linking.

Due to its extremely high molecular weight (2–6 million grams per mole), the melt viscosity of UHMWPE is very high, making it practically impossible to process by using conventional processing methods such as injection molding. Currently, compression molding and ram extrusion are two major processing methods to

consolidate UHMWPE resins into bars or rods [5]. However, processing parameters [6] affect the wear and fatigue properties of UHMWPE, which are crucial for its performance as a load-bearing surface in the joint implants [7,8].

During *in vivo* articulation against (commonly) cobalt-chrome alloy in a total joint implant, UHMWPE components experience cyclic compressive and tensile loading, and abrasive and adhesive shear [9]. Stresses are dissipated through plastic deformation of the polymer, but can also concentrate at structural defects (e.g., crack), causing fatigue crack propagation and increasing risk of fracture [10,11]. Current processing methods, while providing reproducible and adequate mechanical properties for medical implants, inevitably leave structural defects inside the UHMWPE components due to the high viscosity and very slow self-diffusion of UHMWPE chains [10,11]. Although type 1 fusion defects (incomplete inter-particle voids) can be removed by properly controlling the consolidation conditions, type 2 fusion defects (incomplete inter-particle cohesion by self-diffusion) are common in UHMWPE. The interface of type 2 fusion defects may have less toughness than that of bulk UHMWPE [12] and thus could be potential sites for failure under cyclic loading. Moreover, such defects could be readily exaggerated by subsequent treatments such as radiation cross-linking for wear reduction [3] and high pressure crystallization for improved strength [13] due to the contraction of the polymer networks, which can lead to a further decrease in the strength and/or toughness of the material.

* Corresponding author. Harris Orthopaedic Laboratory, Massachusetts General Hospital, GRJ 1206, Boston, MA 02114, United States. Tel.: +1 617 7260657; fax: +1 617 6432521.

E-mail address: eoral@partners.org (E. Oral).

One major reason for the existence of structural defects in consolidated UHMWPE is the extremely slow diffusion of the ultra long polyethylene chains during consolidation. According to the Reptation Theory by de Gennes [14] and the tube model of Doi-Edwards [15], the motion of a single linear chain is described as restricted by the topological constraints ('tube') from the neighboring chains so that this chain can only relax along the tube axis. Dynamic thermal analysis of entangled UHMWPE (molecular weight, 3.6×10^6 g/mol) showed a terminal relaxation time of 15 h at 180 °C [16], much longer than the conventional processing time (usually less than 1 h at 190–250 °C). At the boundaries of the resin powder particles where there were no entanglements at all before consolidation, chain diffusion may need longer time to establish adequate entanglements. Therefore, it is not surprising that the granules "fused" at the current processing conditions contain fusion defects. Since the self-diffusion coefficient (D) [17] increases with increasing temperature ($D \sim \exp(C/T)$, where C is a constant), it is possible to accelerate the self-diffusion by melting UHMWPE at higher temperatures to remove the fusion defects.

Therefore, we hypothesized that the strength and toughness of UHMWPE could be improved by enhancing chain diffusion across fusion boundaries after consolidation, which could be enabled at elevated temperatures above the melting point. To test this hypothesis, we determined the tensile mechanical properties and IZOD impact strength of UHMWPEs processed at 280, 300 and 320 °C after consolidation. We also investigated the effects of high temperature melting and associated structural changes on the wear resistance of UHMWPE by using bi-directional pin-on-disc wear testing.

2. Experiments

2.1. Thermogravimetric analysis (TGA)

In order to assess the thermal stability of UHMWPE at high temperatures, TGA was performed by using a Q-500 Thermogravimetric analyzer (TA Instruments Inc., Newark, DE). One sample (about 10 mg) was loaded on the pan and heated up to a target temperature (280, 300, 320, 340, and 400 °C) at 20 °C/min and held at the temperature for 1440 min under nitrogen flow at 60 ml/min. The weight over time was sampled every 30 s. The remaining weight percentage was plotted against time to compare the thermal stability of UHMWPE at different temperatures.

2.2. High temperature melting (HTM) of compression molded UHMWPE

Compression molded GUR 1050 UHMWPE (CM UHMWPE) (Orthoplastics, Bacup Lancashire, UK) with dimensions of $250 \times 60 \times 45$ mm³ (length \times width \times height) were melted in a programmable inert gas convection oven (Despatch Industries, Minneapolis, MN) under continuous nitrogen flow (flow rate was 2 m³/min). The oven was preheated to a preset temperature with nitrogen purge. Then, the UHMWPE blocks were placed in the oven and purged again. Three temperatures (280, 300, and 320 °C) were used to melt the UHMWPE. At each temperature, the UHMWPE was held for 2, 5, or 12 h and then cooled down to 40 °C within 2 h (or an average cooling rate of 2.5 °C/min or less). The samples were held at 40 °C for 20 min in the oven before retrieval. Such melted UHMWPE was denoted as HTM UHMWPE. Specifically, the HTM UHMWPE samples were denoted as UH T–t, where T is the melting temperature and t is the melting duration; for example UH 280–2, UH 280–5, and UH 280–12 represent UHMWPE melted at 280 °C for

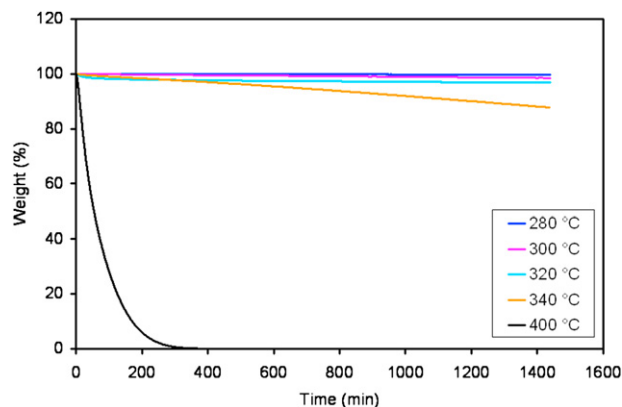


Fig. 1. TGA curves of UHMWPE melted at 280, 300, 320, 340, and 400 °C for 24 h.

2, 5, and 12 h, respectively. Compression molded UHMWPE was melted at 180 °C for 5 h to remove its thermal history and used as control.

2.3. Tensile testing

Thin sections (thickness = 3.2 mm) were machined (Eastern Tool Inc, Medford, MA) from HTM UHMWPE and CM UHMWPE. Tensile testing specimens (Type V, $n = 5$) were stamped from these thin sections according to ASTM D638. Uni-axial tensile testing was conducted by using an MTS machine (Eden Prairie, MN) at a crosshead speed of 10 mm/min. The axial displacement and force were sampled at a rate of 100 Hz. The extension of a specific gauge on the specimen was measured by a laser extensometer, which was used to determine the elongation at break (EAB).

True stress–true strain curves were converted from the engineering stress–strain results by using the extension readings from the laser extensometer. The ultimate tensile strength (UTS), yield strength (YS), work-to-failure (area under the engineering stress–strain curve; WF), and elastic modulus (E) were calculated. Statistical analysis was performed by using a Student's t -test for two-tailed distributions with unequal variance where applicable.

The strain-hardening modulus (G) is regarded as the intrinsic property of an entangled amorphous network. According to the Gaussian model by Haward and Thackray [18], the true stress (σ) and G are related by

$$\sigma = G(\lambda^2 - 1/\lambda) + Y \quad (1)$$

where λ is the extension ratio and $\lambda = \exp(\epsilon_t)$ with ϵ_t as true strain, and Y is the flow stress exerted by the crystalline phase including intra- and interlamellar coupling. In order to calculate the strain-hardening modulus of the amorphous phase in this semi-crystalline polymer, we deduced the Haward plots from the true stress–strain curves and extracted the slope of the fitted line after yielding.

Table 1

Percentage weight loss of UHMWPE at different temperature and for different durations.

Temperature (°C)	Weight loss at different durations (%)			
	2 h	5 h	12 h	24 h
280	0.05	0.1	0.24	0.28
300	0.2	0.4	1.3	1.5
320	1.8	2.2	3.1	3.2
340	1.1	2.3	10.2	12.3

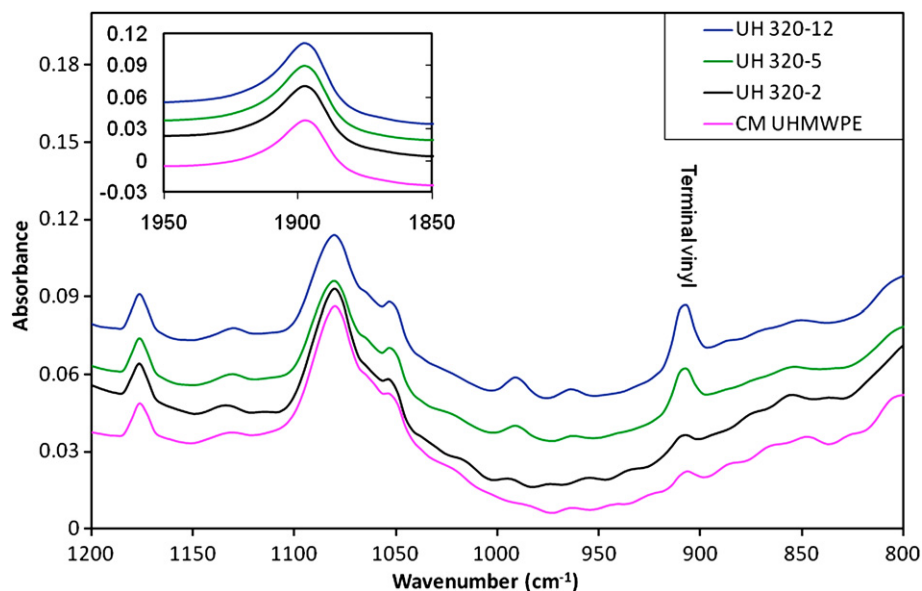


Fig. 2. FTIR spectra of UHMWPE melted at 320 °C for 0, 2, 5, and 12 h. The peaks at 909 and 990 cm^{-1} increase with melting time. The inset shows the corresponding IR absorbance at 1895 cm^{-1} used as reference for vinyl indexing.

2.4. Double-notched Izod impact strength measurements

Double-notched Izod impact strength measurements were conducted at Orthoplastics Inc. (Bacup Lancashire, UK). The specimens ($n = 5$ for each material) were machined to $63.5 \times 12.7 \times 6.35 \text{ mm}^3$ bar and double notched to a depth of $4.57 \pm 0.08 \text{ mm}$ according to ASTM F648. The specimens were conditioned after notching for not less than 16 h at $23 \pm 2 \text{ }^\circ\text{C}$ and tested in accordance with ASTM F648. The energy absorbed by the specimens was recorded for the calculation of the impact strength in kJ/m^2 .

2.5. Peak melting points and percentage crystallinity

The peak melting points and percentage crystallinity were determined by using a Q-1000 Differential Scanning Calorimeter (TA Instruments, Newark, DE) that had been calibrated with indium. Three specimens of each material were weighed with a Sartorius CP 225D balance to a resolution of 0.01 mg and placed in standard aluminum pans. The pan was crimped with an aluminum

lid and put in the heating cell, together with an aluminum reference. With a nitrogen flow at 50 ml/min, the cell temperature was ramped from $-20 \text{ }^\circ\text{C}$ to $180 \text{ }^\circ\text{C}$ at $10 \text{ }^\circ\text{C/min}$, then from $180 \text{ }^\circ\text{C}$ to $20 \text{ }^\circ\text{C}$ at $-10 \text{ }^\circ\text{C/min}$, and finally from $-20 \text{ }^\circ\text{C}$ to $180 \text{ }^\circ\text{C}$ at $10 \text{ }^\circ\text{C/min}$ again. Before each cycle, the cell temperature was held at each start temperature for 2 min. Thus, three traces were recorded as heat flow versus temperature. The cycles are referred to as 1st heat, 1st cool, and 2nd heat, respectively.

The percentage crystallinity of each sample was calculated by integrating the enthalpy peak from 20 to $160 \text{ }^\circ\text{C}$ and normalizing it with the fusion enthalpy of 100% crystalline polyethylene (291 J/g). The percentage crystallinity was calculated by averaging the values of three specimens of each material.

2.6. Determination of terminal vinyl content by Fourier Transform Infrared Spectroscopy (FTIR)

In order to evaluate the chain scission in UHMWPE by high temperature melting, the melted samples were microtomed into thin slices (thickness = $150 \text{ }\mu\text{m}$) by using an LKB Sledge Microtome (Sweden). FTIR absorption spectra of these thin slices were collected by using a UMA-500 infrared microscope (Bio-Rad)

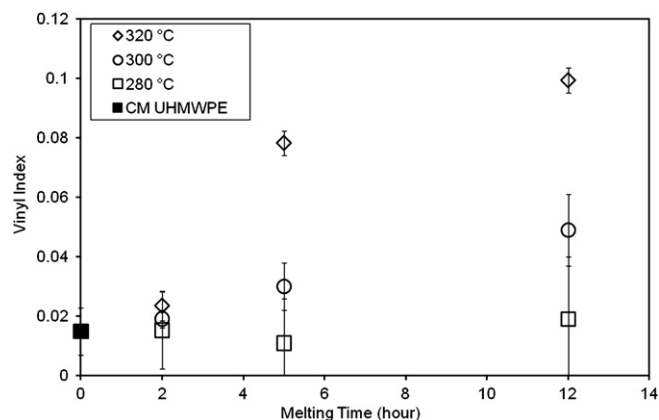


Fig. 3. The terminal vinyl index as a function of melting time at 280, 300, and $320 \text{ }^\circ\text{C}$, in comparison with CM UHMWPE that was not subjected to high temperature melting.

Table 2
Thermal properties of UHMWPE after high temperature melting.

Sample Code	Description	T_m ($^\circ\text{C}$)		X_c (%)		T_c ($^\circ\text{C}$)
		1st heat	2nd heat	1st heat	1st cool	
CM UHMWPE	no melting	135.1 ± 0.1	133.0 ± 0.1	51.9 ± 2.9	118.8 ± 0.3	
CM-180	$180 \text{ }^\circ\text{C}$, 5 h	134.2 ± 0.3	132.1 ± 0.4	54.2 ± 0.6	117.7 ± 0.4	
UH 280-2	$280 \text{ }^\circ\text{C}$, 2 h	133.7 ± 0.2	132.3 ± 0.2	55.2 ± 1.3	118.0 ± 0.3	
UH 280-5	$280 \text{ }^\circ\text{C}$, 5 h	133.1 ± 0.1	133.0 ± 0.1	54.5 ± 0.7	117.0 ± 0.5	
UH 280-12	$280 \text{ }^\circ\text{C}$, 12 h	133.5 ± 0.2	132.3 ± 0.3	56.5 ± 0.9	117.7 ± 0.1	
UH 300-2	$300 \text{ }^\circ\text{C}$, 2 h	133.6 ± 0.1	132.3 ± 0.05	56.9 ± 1.7	117.5 ± 0.4	
UH 300-5	$300 \text{ }^\circ\text{C}$, 5 h	134.0 ± 0.1	133.0 ± 0.4	60.5 ± 0.4	117.4 ± 0.2	
UH 300-12	$300 \text{ }^\circ\text{C}$, 12 h	133.7 ± 0.1	132.6 ± 0.2	61.9 ± 1.4	115.4 ± 0.4	
UH 320-2	$320 \text{ }^\circ\text{C}$, 2 h	133.9 ± 0.3	132.6 ± 0.04	60.6 ± 0.3	117.1 ± 0.5	
UH 320-5	$320 \text{ }^\circ\text{C}$, 5 h	134.1 ± 0.2	132.9 ± 0.4	61.9 ± 2.1	114.3 ± 0.2	
UH 320-12	$320 \text{ }^\circ\text{C}$, 12 h	133.7 ± 0.2	132.9 ± 0.7	63.5 ± 2.6	114.6 ± 1.4	

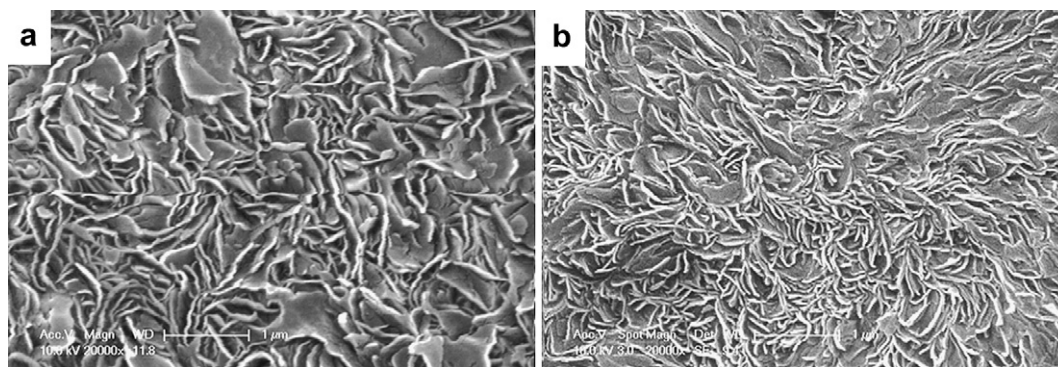


Fig. 4. SEM images of CM UHMWPE (a) before and (b) after melting at 300 °C for 5 h. The crystalline lamellae were exposed by etching of the amorphous phase.

Laboratories, Natick, MA) scanning from 400 to 4000 cm^{-1} (step width 2 cm^{-1}) in transmission mode. Chain scissioning taking place in UHMWPE at high temperatures led to the formation of terminal vinyl groups with absorbance at 909 and 990 cm^{-1} . The content of these terminal vinyl groups was indexed by normalizing the integral of the peak at 909 cm^{-1} against that of the polyethylene skeleton peak at 1895 cm^{-1} . These vinyl indices were taken as an indication to the extent of chain scission occurring in UHMWPE under high temperatures.

2.7. Freeze-fracturing and scanning electron microscopy (SEM)

Both HTM and CM UHMWPEs (approximately $60 \times 10 \times 10 \text{ mm}^3$) were pre-cracked with a razor blade and immersed in liquid nitrogen for 2 h before they were fractured. The fracture surface was coated with gold (Cressington Sputter Coater, Ted Pella Inc, Redding, CA) for SEM observation under an FEI/Philips XL30 FEG ESEM at 10 kV. In order to investigate the crystal structures, the fracture surface was etched in an etching solution (1% KMnO_4 in a mixture of 95% H_2SO_4 and 85% H_3PO_4 at a volume ratio of 2:1) at 80 °C for 4 h with sonication in order to remove the amorphous phase. The samples were then completely rinsed with de-ionized water, dried, and sputtered with gold for SEM investigation.

2.8. Bi-directional pin-on-disc (POD) wear test

The bi-directional POD wear test was performed on an MTS machine (Eden Prairie, MN) in bovine serum. Pins of 13-mm length and 9-mm diameter ($n = 3$ for each material) were machined and mounted on the MTS wear tester to undergo bi-directional motions on polished CoCr discs at 2 Hz and a step length of $5 \times 10 \text{ mm}$ under a maximum load of 1.9 kN. The pins were weighed at every 157

kilo-cycle until a total of 1 million cycles (MC) and the weight loss from 0.5 to 1 MC were used to evaluate the gravimetric wear rate in milligram per million cycles (mg/MC).

3. Results

TGA results demonstrated that UHMWPE decomposed and lost its weight quickly at 400 °C (Fig. 1). The UHMWPE weight loss for different durations at 340, 320, 300, and 280 °C is tabulated in Table 1. The weight loss at temperatures below 320 °C for durations shorter than 12 h was 3.1% or less, indicating that there were not much volatile residues generated in UHMWPE at these temperatures. Thus, we adopted three temperatures (280, 300, and 320 °C) in this work to investigate the effect of high temperature melting on the structure, morphology, and mechanical properties of UHMWPE.

At high temperatures, polyethylene undergoes chain scission through the breaking of the carbon–carbon bonds along its backbone, leading to the formation of terminal vinyl groups [19–21]. The vinyl groups were indexed by using the absorbance at 909 cm^{-1} (Fig. 2) to characterize the extent of chain scissioning. UHMWPE contains more than one terminal vinyl group per chain [22] and this content did not change significantly during melting at 280 °C for up to 12 h ($p = 0.84$ for the vinyl index at 12 h compared to CM UHMWPE; Fig. 3). As the temperature was increased to 300 and 320 °C, the vinyl index increased significantly ($p = 0.001$ and 0.000002 for 300 and 320 °C at 12 h compared to CM UHMWPE; Fig. 3), indicating the formation of new vinyl groups via chain scissioning.

High temperature melting decreased the peak melting point (T_m) of UHMWPE from 135 °C to 133–134 °C, but increased the crystallinity (X_c) with increasing temperature and duration (Table 2). This decrease in T_m is indicative of the formation of thinner

Table 3

Tensile properties, double-notched Izod impact strength, and bi-directional pin-on-disc (POD) wear rate of high temperature melted UHMWPE.

Materials	UTS (MPa)	<i>p</i>	YS (MPa)	WF (kJ/m ²)	E (GPa)	EAB (%)	Izod impact strength (kJ/m ²)	<i>p</i>	POD wear rate (mg/MC)	<i>p</i>
CM UHMWPE	59 ± 4.5	1	21 ± 0.8	3242 ± 444	1.3 ± 0.3	401 ± 15	127 ± 6.7	1	10.2 ± 0.9	1
CM-180-5	48 ± 1.1	0.005	20 ± 0.6	2500 ± 64	1.9 ± 0.1	420 ± 6	N.A.	N.A.	N.A.	N.A.
UH 280-2	56 ± 1.2	0.28	20	3314 ± 167	1.6 ± 0.5	444 ± 1	N.A.	N.A.	N.A.	N.A.
UH 280-5	52 ± 6.3	0.11	20 ± 0.5	3120 ± 637	1.4 ± 0.8	473 ± 36	N.A.	N.A.	10.7 ± 1.1	0.29
UH 280-12	55 ± 4.7	0.31	20 ± 0.6	3673 ± 550	1.6 ± 0.1	513 ± 16	175 ± 9.5	0.00005	11.2 ± 0.3	0.17
UH 300-2	53 ± 3.3	0.07	20	3266 ± 379	1.4 ± 0.2	457 ± 20	123 ± 5.8	0.37	11.2 ± 2.3	0.55
UH 300-5	60 ± 3.3	0.64	21 ± 0.6	4691 ± 653	1.6 ± 0.3	546 ± 37	140 ± 3.9	0.02	11.3 ± 0.7	0.17
UH 300-12	60 ± 4.5	0.64	22 ± 0.6	6646 ± 991	1.6 ± 0.2	752 ± 23	111 ± 4.5	0.009	12.5 ± 1.1	0.05
UH 320-2	60 ± 2.2	0.50	21 ± 0.5	4638 ± 1133	1.3 ± 0.1	521 ± 24	139 ± 18.8	0.25	9.7 ± 2.7	0.78
UH 320-5	53 ± 1.9	0.05	22 ± 0.5	6651 ± 263	1.9 ± 0.1	974 ± 46	94 ± 3.7	0.0005	10.1 ± 0.1	0.88
UH 320-12	43 ± 2.0	0.0006	23 ± 0.6	5726 ± 505	2.8 ± 0.6	1061 ± 71	66 ± 5.4	8.5×10^{-6}	15.6 ± 2.5	0.05

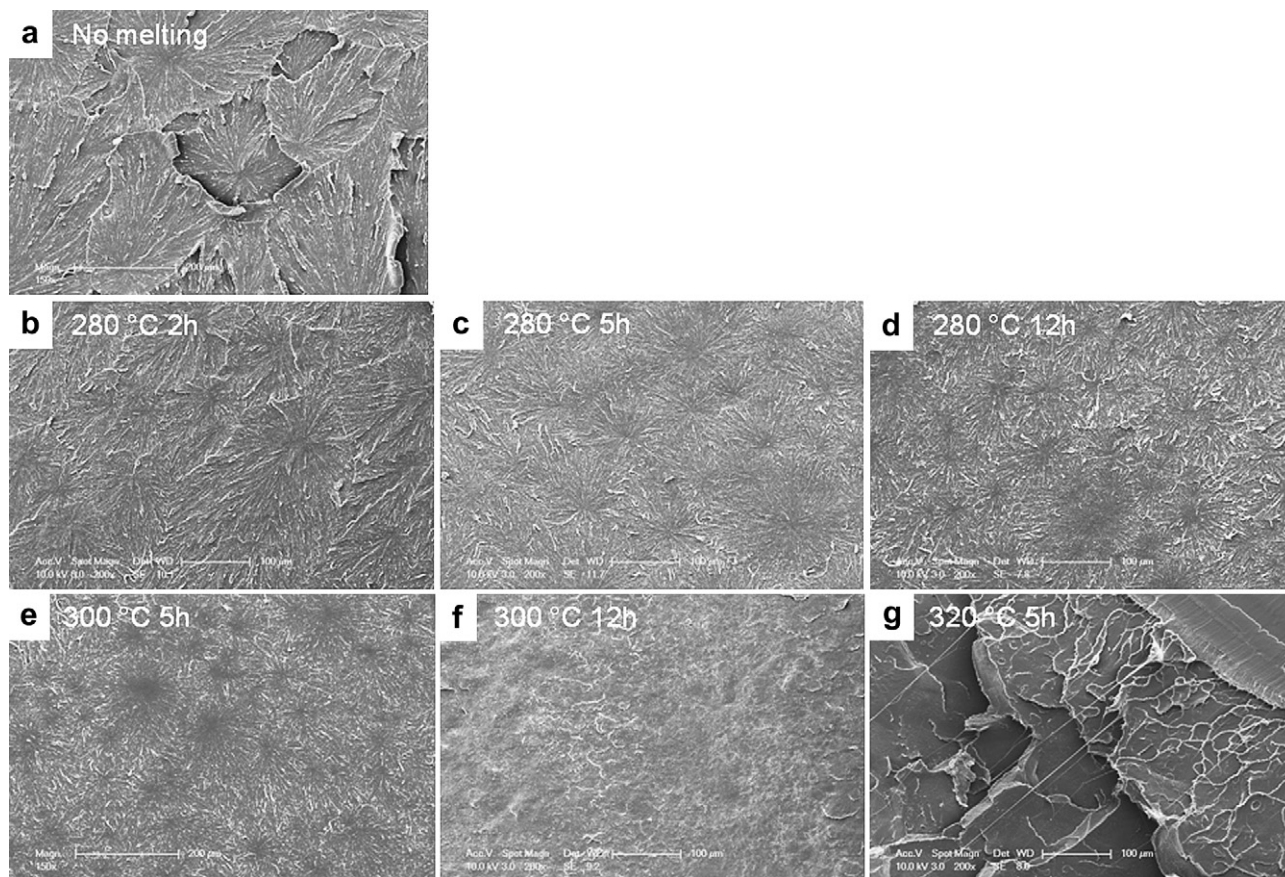


Fig. 5. Representative SEM images of the freeze-fracture surfaces of (a) CM UHMWPE and after melting at (b) 280 °C for 2 h, (c) 280 °C for 5 h, (d) 280 °C for 12 h, (e) 300 °C for 5 h, (f) 300 °C for 12 h, (g) 320 °C for 5 h.

crystalline lamellae. HTM UHMWPE with the amorphous phase etched away showed thinner crystalline lamellae (Fig. 4b), in comparison to the lamellae of CM UHMWPE (Fig. 4a). The crystallization temperature (T_c) at the first cool cycle was decreased from 118 °C for CM UHMWPE to as low as 114 °C for HTM UHMWPE melted at higher temperatures and for longer durations (Table 2).

High temperature melting significantly increased the elongation at break (EAB), from 401% for CM UHMWPE up to 1061% for UH 320-12 (melted at 320 °C for 12 h, Table 3). At the same time, the work-to-failure (WF) was significantly increased ($p < 0.05$) for the UH 300-5, UH 300-12, UH 320-5, and UH 320-12, in comparison with CM UHMWPE. In contrast, the ultimate tensile

strength (UTS) did not significantly change after HTM, except for that melted at 320 °C for 12 h that showed a significant decrease in UTS (Table 3). The yield strength and Young's modulus were not significantly influenced by the HTM processing except at 320 °C for 5 h and 12 h, where the modulus increased significantly compared to CM UHMWPE ($p = 0.007$ and 0.001 , respectively).

The impact strength was increased from 127 ± 6.7 kJ/m² before HTM to 175 ± 9.5 kJ/m² for UH 280-12 ($p = 0.00005$), 140 ± 3.9 kJ/m² for UH 300-5 ($p = 0.02$), and 139 ± 18.8 kJ/m² for UH 320-2 ($p = 0.25$). However, at higher temperatures and/or for longer durations, the impact strength was significantly ($p \ll 0.05$) decreased (Table 3).

Bi-directional POD wear tests (Table 3) of the HTM and CM UHMWPE demonstrated that HTM did not significantly change the POD wear rate, except for the UH 320-12, of which the POD wear rate was increased to 15.6 ± 2.5 mg/MC ($p = 0.05$).

4. Discussion

In this work, we have demonstrated that high temperature melting after consolidation improved the tensile and impact toughness of UHMWPE. The structural and morphological changes as determined by FTIR, DSC and SEM revealed that chain scissioning and increased self-diffusion should account for the increasing toughness after high temperature melting. Increased toughness associated with high temperature melting did not significantly sacrifice the wear resistance, which is surprising in view of the significant increases in plasticity observed as a result of high temperature melting.

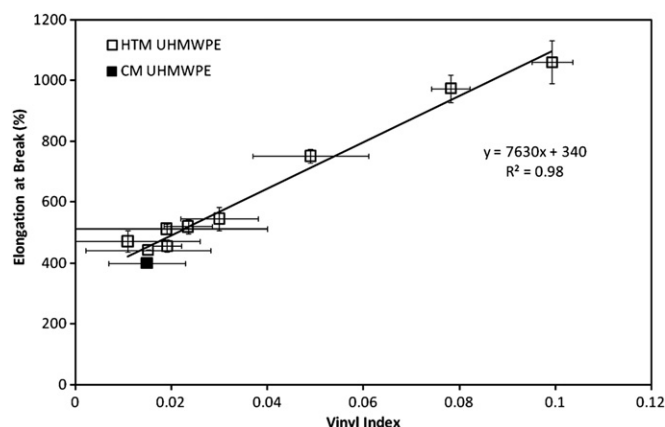


Fig. 6. Dependence of elongation at break on the terminal vinyl group index.

At high temperatures, two major processes could affect the morphology and properties of UHMWPE: One is the increased self-diffusion of chain entanglements across the granule boundaries and the other is the chain scissioning, which in turn would help self-diffusion. Increased self-diffusion is evident in the morphology of the freeze-fractured surfaces of HTM UHMWPE compared to CM UHMWPE (Fig. 5). Consolidated UHMWPE showed fused granules with apparent diameters of 200 μm or larger and these granules share explicit boundaries with defects (Fig. 5a). Melting at 280 $^{\circ}\text{C}$ for 2 h decreased such fusion defects and the granules became smaller (Fig. 5b). The granule size decreased further with increasing melting duration to 5 and 12 h at 280 $^{\circ}\text{C}$ (Fig. 5c,d) and also at higher temperatures (e.g., 300 $^{\circ}\text{C}$, Fig. 5e). When melted at 300 $^{\circ}\text{C}$ for 12 h, there were no clear granule boundaries under SEM.

Incidentally, the work-to-failure of this sample was among the highest (Table 3). Further increasing the melting temperature to 320 $^{\circ}\text{C}$ at 5 h yielded super-ductile UHMWPE so that the sample frozen in liquid nitrogen did not experience brittle fracture. Instead, the fracture surface featured ductile tears and very long fibers (Fig. 5g). Therefore, the elimination of granule boundaries (and structural defects) may be one reason that accounts for the increases in the tensile and impact strengths (Table 3). These results supported our hypothesis that HTM can increase the strength and toughness of UHMWPE by improving inter-granule diffusion and eliminating the internal structural defects.

The improved fusion and entanglements during HTM provide additional constraints to the crystallization of UHMWPE chains when cooled down from the melt and thus lead to the formation of

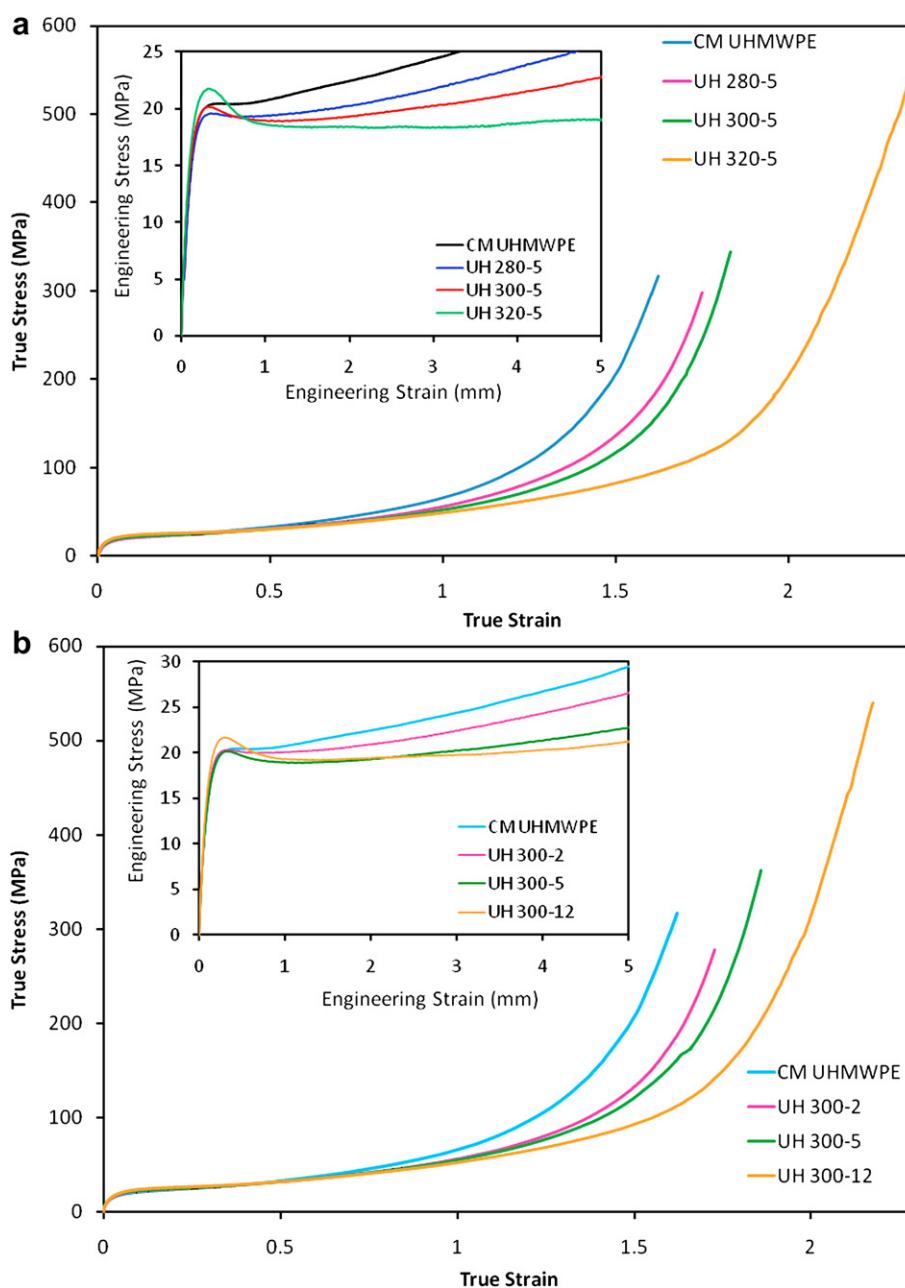


Fig. 7. True stress-strain curves of UHMWPE melted (a) at 280, 300, and 320 $^{\circ}\text{C}$ for 5 h, and (b) at 300 $^{\circ}\text{C}$ for 2, 5, and 12 h. The insets in (a) and (b) show the yielding portion of corresponding engineering stress-strain curves.

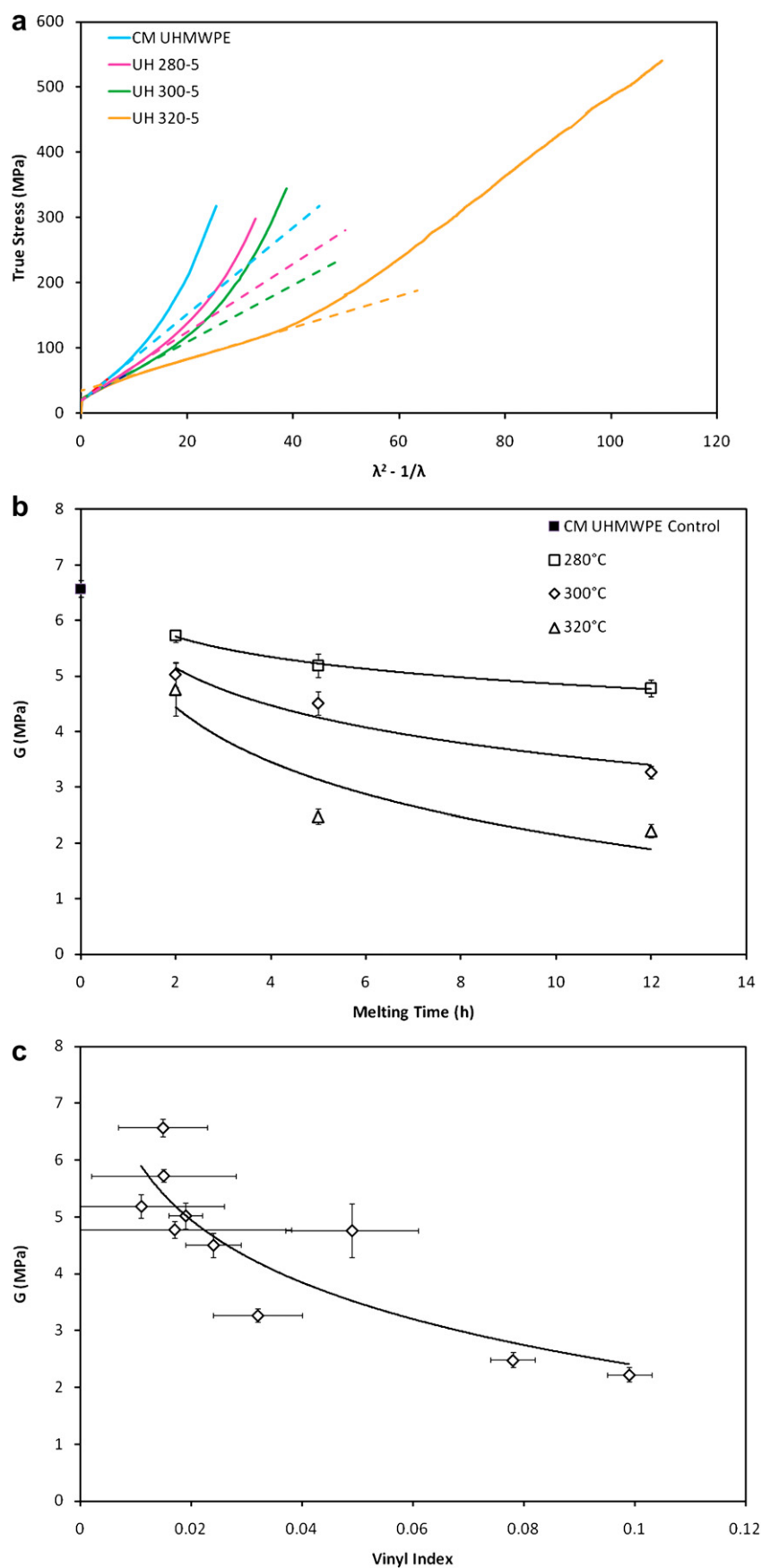


Fig. 8. (a) Representative Haward plots derived from the true stress-strain curve of UHMWPE melted at 280, 300, and 320 °C for 5 h. The slopes of the dashed fitted lines represent the strain-hardening modulus, G . (b) The strain-hardening modulus as a function of melting time at 280, 300, and 320 °C. (c) The strain-hardening modulus as a function of vinyl index.

thinner lamellae, as evident in Fig. 4. At the same time, the crystallization temperature of HTM UHMWPE was decreased from 118 °C down to 114 °C with increasing HTM temperature (Table 2), which suggested that a higher degree of undercooling was needed for the crystallization of HTM UHMWPE chains compared to CM UHMWPE chains, presumably due to the enhanced entanglements during high temperature melting.

The second effect of HTM, namely chain scissioning, would form vinyl end groups [19,20], which were confirmed by determining the increase in the vinyl index with melting time and temperature (Fig. 3). Thus formed shorter chains may be the reason for increased recrystallization (Table 2) and may also explain the increased elongation of UHMWPE (Fig. 6). Another factor that may have contributed to increased elongation is the plastic deformation of crystals [23]. In fact, after yielding, the deformation of semi-crystalline polymers under tensile loading is believed to cause the orientation of the amorphous network and the slippage of the crystal lamellae [23,24]. In comparison to the CM UHMWPE crystals, the thinner crystals in HTM UHMWPE could be more liable to breaking and slip under uni-axial stress. Besides, the polymer network with enhanced entanglements and shorter chains could experience more slipping and orientation under load than the networks in CM UHMWPE, thus enhancing the elongation at break.

The increased crystal plasticity was reflected by the deep necking after yielding in the engineering stress–strain curves (Fig. 7a and b, insets) and the decreased strain-hardening modulus, G , in the HTM UHMWPE as a function of increased temperature and time at melting temperature (Fig. 8b). Since chain scissioning was increased with increasing melting time and temperature, Fig. 8b essentially reflects the effect of chain scission on G , which decayed with increasing vinyl index (Fig. 8c). The decrease in the strain-hardening modulus indicates an increase in the plasticity of the crystals [25] (that allows for more plastic deformation under stress). We observed whitening in samples that were extended to strains larger than 600% (Fig. 9), indicative of significant deformation of the crystalline lamellae accompanied by cavitation and high amounts of strain-induced recrystallization.

Interestingly, the UTS was only significantly decreased at vinyl index levels above 0.06 (Table 1 and Fig. 10a) compared to CM UHMWPE. In contrast, the work-to-failure increased up to 6600 kJ/m² with increasing vinyl index below an index level of 0.06 (Fig. 10b). HTM did not increase the tensile strength of UHMWPE, but the elimination of structural defects, the increased entanglements and plasticity allowed for more energy dissipation before breaking under uni-axial tensile loading. That is, the tensile toughness of UHMWPE was remarkably increased by HTM.

In contrast to the UTS and work-to-failure, the Izod impact strength was more sensitive to chain scissioning. It was increased sharply from 127 kJ/m² for conventional UHMWPE to 175 kJ/m² for UH 280-12 (Table 3, Fig. 11). According to the vinyl index values, there was not much chain scissioning at 280 °C at 12 h (Fig. 3). At this stage, presumably enhanced chain entanglements dominated. Further chain scissioning at higher temperatures and for longer durations led to a rapid decrease in the impact toughness (Fig. 11). At vinyl index larger than 0.05, the impact strength became significantly lower than that of the CM UHMWPE.

We would point out that the high temperature melting is different from melting above T_m of UHMWPE that removes the thermal history associated with the consolidation process of UHMWPE. Melting CM UHMWPE at 180 °C for 5 h, for example, removed its thermal history and reduced the T_m to 134.2 °C and increased the crystallinity to 54.2%, in comparison to CM UHMWPE (Table 2). These small changes significantly decreased the mechanical strength (Table 3). In contrast, high temperature melting caused a significant decrease in the T_m and increased the

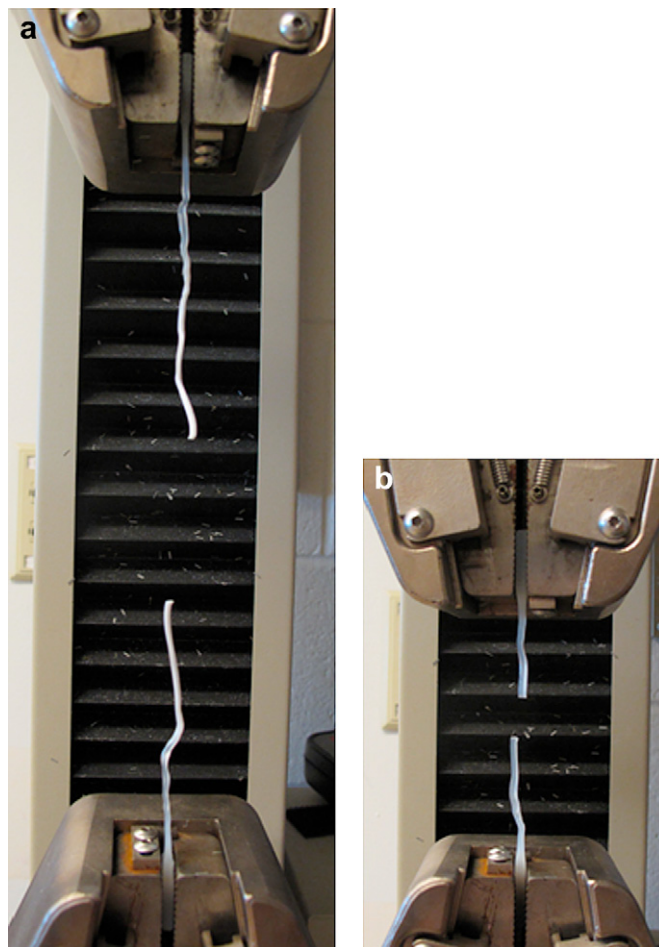


Fig. 9. (a) A photograph of the whitening of a UH 300-12 tensile sample fractured at high strain in comparison to CM UHMWPE (b).

crystallinity. Moreover, the UTS, WF, and EAB were also improved by high temperature melting, compared to the thermal history removed CM UHMWPE by melting at 180 °C.

We attribute the elimination of structural defects through the self-diffusion of the UHMWPE chains for the increase in the tensile toughness (WF) and the impact strength. At conventional molding temperatures ($T_p < 200$ °C), self-diffusion is very slow and the time required for the UHMWPE chains to reptate [14] through the highly viscous UHMWPE melt (> 15 h) [16] is much longer than the typical molding time (≤ 0.5 h). In particular, it is more difficult for the chains to reptate across the granule boundaries, where there are no entanglements before molding. This explains the presence of the granule with explicit boundaries (Fig. 5a) on the freeze-fractured surface of the as-molded CM UHMWPE. These boundaries could serve as structural defects with low toughness that may lead to the initiation of cracks under cyclic loading.

At high temperatures, the melt viscosity is reduced and the chain mobility is enhanced, whereas some UHMWPE chains were cleaved. As a result, self-diffusion via chain reptation through the tube defined by the neighboring chains [15] is accelerated. Thus, the granules further fused and the chain entanglements were improved, leading to the formation of spherulites without distinct boundaries after recrystallization (Fig. 5b). The structural defects were eliminated and the stress concentration could be largely reduced.

Besides the mechanical strength and toughness, wear is another important issue for UHMWPE as a material for articulating surfaces

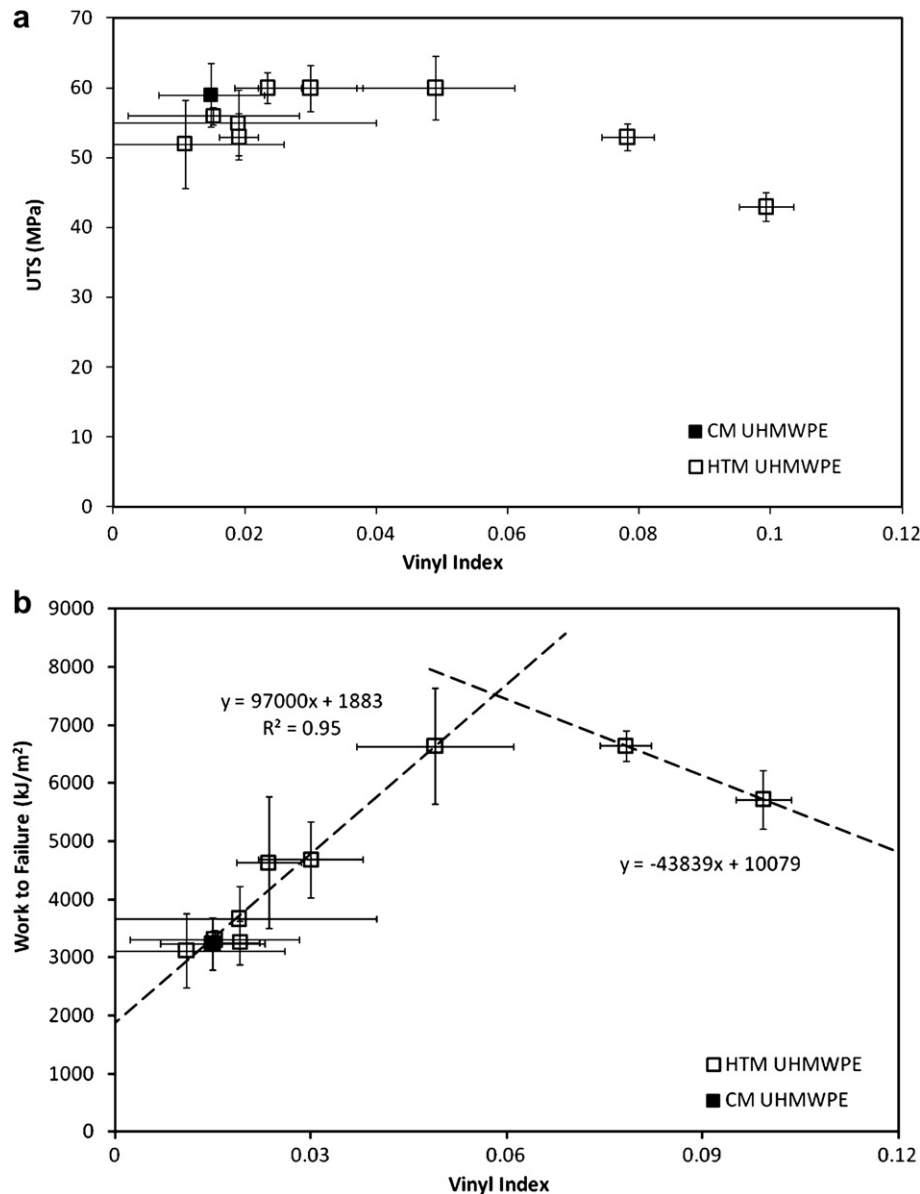


Fig. 10. Effect of chain scissioning (vinyl index) on (a) the ultimate tensile strength and (b) the work-to-failure of high temperature melted UHMWPE. The solid square represents the properties of CM UHMWPE, which was not subjected to high temperature melting.

in vivo, especially since wear has been linked to a plasticity-induced damage layer on articular surfaces of components [26]. Under multi-axial articulation, polyethylene experiences yielding, plastic deformation, strain softening, orientation, and weakening in transverse directions, which results in wear [27]. Radiation cross-linking has been effective in reducing wear by decreasing the plasticity of polyethylene [28]. Melting UHMWPE at very high temperatures in this work substantially increased the plasticity of the polymer, as indicated by the increased elongation (Fig. 6), but the wear rates of UHMWPE after HTM were not significantly increased by HTM, except for UH 320-12 that experienced severe chain scissioning (Fig. 12).

According to the mechanisms for adhesive wear mentioned above, since HTM did not significantly change the yield strength of UHMWPE (Table 3), and significantly improved toughness (work-to-failure, and Izod impact strength) through increased plasticity, the wear rate of HTM would be expected to be significantly increased. However, the wear rate was not substantially influenced

despite increases in the elongation at break on the order of 200%. Thus, these results suggest that for these samples, there are other mechanisms beneficially affecting wear rate. In future work, we propose to improve the wear resistance by radiation cross-linking HTM UHMWPE. Both the chain entanglements and the covalent cross-links are expected to work together to provide low wear, high elongation, and improved toughness, in comparison to the cross-linked UHMWPE without previous high temperature melting.

By inducing chain scissioning and improving chain entanglements at properly selected high temperature melting conditions, it was possible to improve the ductility and impact toughness without significantly sacrificing the yield strength, ultimate tensile strength, and wear resistance. The gain in the plasticity due to chain scissioning and increased crystal plastic deformation did not significantly increase the wear rate. Therefore, high temperature melting is a feasible method of improving the strength of UHMWPE without detrimentally affecting its wear resistance. Thus, it has the potential of compensating for the reduction in the mechanical

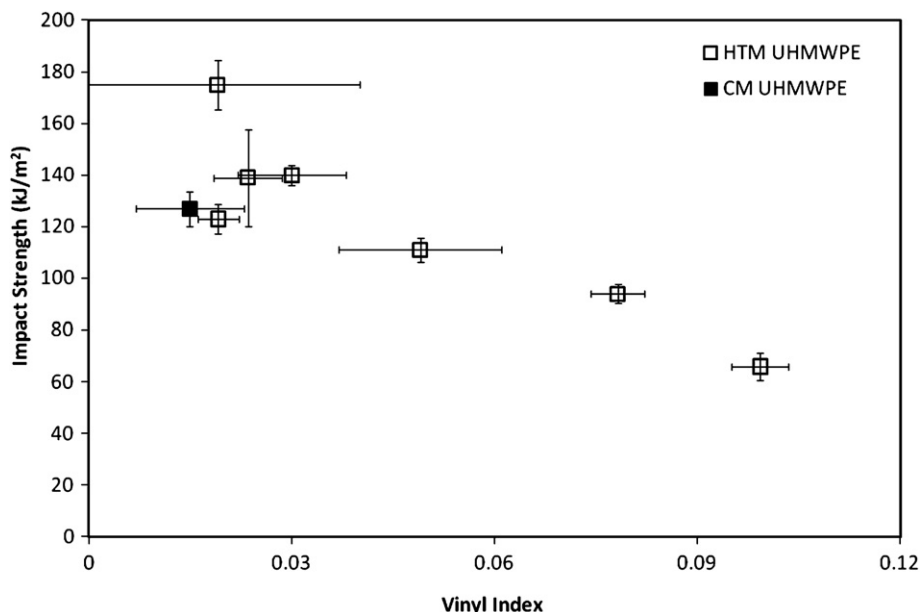


Fig. 11. Effect of chain scissioning (vinyl index) on double-notched Izod impact strength of high temperature melted UHMWPE. The solid square represents the impact strength of CM UHMWPE.

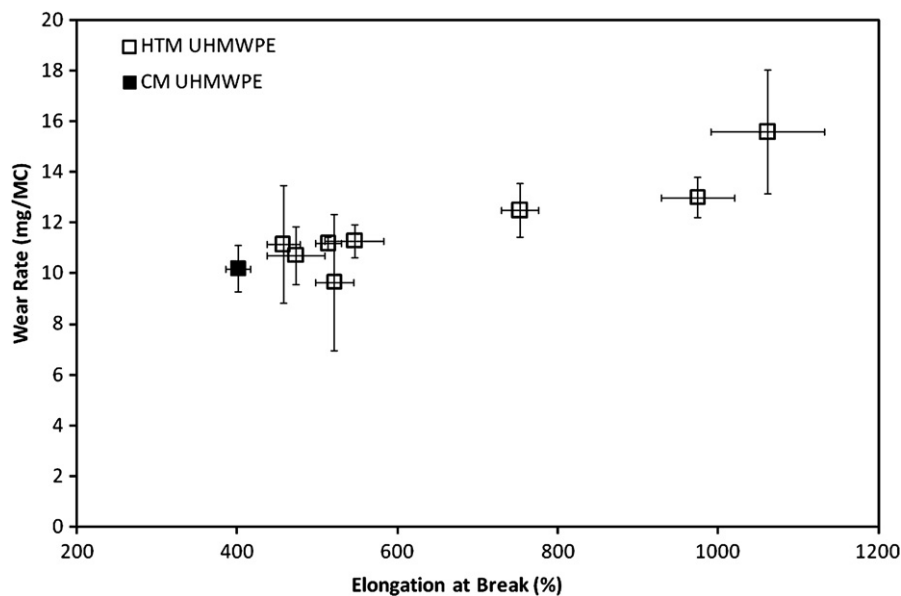


Fig. 12. The bi-directional pin-on-disc wear rate of high temperature melted UHMWPE as a function of elongation at break. The solid square represents the wear rate of CM UHMWPE.

properties of the polymer caused by subsequent cross-linking to decrease wear.

5. Conclusion

High temperature melting of consolidated UHMWPE was effective in improving its toughness by using properly selected melting temperatures and durations. The chain scissioning and improved chain entanglements through granule boundaries were two major causes for the improvement of the mechanical properties. The improved plasticity and ductility by HTM did not significantly compromise the wear rates.

Acknowledgements

The authors are grateful to Dr. Neil Hubbard, Mark Allen, and Rebecca Field of the Orthoplastics Inc., UK for assistance in the double-notched Izod impact strength measurements. This study was funded by laboratory funds.

References

- [1] Kurtz S, Hozack WJ, Marcolongo M, Turner J, Rimnac CM, Edidin A. *Journal of Arthroplasty* 2003;18(7 Supp. 1):68–78.
- [2] Bell CJ, Walker PS, Abeyesundera M, Simmons JMH, King PM, Blunn GW. *Journal of Arthroplasty* 1998;13(3):280–90.

- [3] Muratoglu OK, Bragdon CR, O'Connor DO, Jasty M, Harris WH, Gul R, et al. *Biomaterials* 1999;20(16):1463–70.
- [4] Oral E, Wannomae KK, Hawkins NE, Harris WH, Muratoglu OK. *Biomaterials* 2004;25(24):5515–22.
- [5] Kurtz SM. *The UHMWPE handbook*. 1st ed. Amsterdam: Elsevier Academic Press; 2004.
- [6] Gul RM, McGarry FJ, Bragdon CR, Muratoglu OK, Harris WH. *Biomaterials* 2003;24:3193–9.
- [7] Harris WH. *Clinical Orthopaedics and Related Research* 1995;311:46–53.
- [8] Harris WH. *Clinical Orthopaedics and Related Research* 2001;393:66–70.
- [9] Muratoglu O, Mark A, Vittetoe D, Harris W, Rubash H. *Journal of Bone & Joint Surgery* 2003;85-A(1):7–13.
- [10] Wu JJ, Buckley CP, O'Connor JJ. *Biomaterials* 2002;23:3773–83.
- [11] Buckley CP, Wu J, Haughie DW. *Biomaterials* 2006;28:3178–86.
- [12] Haughie DW, Buckley CP, Wu J. *Biomaterials* 2006;28:3875–81.
- [13] Oral E, Godleski Beckos C, Lozynsky A, Malhi A, Muratoglu O. *Biomaterials* 2009;30:1870–80.
- [14] de Gennes P-G. *Scaling concepts in polymer physics*. 4th ed. Ithaca: Cornell University Press; 1979.
- [15] Doi M, Edwards SF. *The theory of polymer dynamics*. Oxford: Clarendon; 1986.
- [16] Rastogi S, Lippits DR, Peters GWM, Graf R, Yao Y, Spiess HW. *Nature Materials* 2005;4:635.
- [17] Bartels CR, Crist B, Graessley WW. *Macromolecules* 1984;17(12):2702–8.
- [18] Haward RN. *Macromolecules* 1993;26:5860–9.
- [19] Oakes WG, Richards RB. *Journal of the Chemical Society*; 1949:2929–35.
- [20] Poutsma ML. *Macromolecules* 2003;36:8931–57.
- [21] Kuroki T, Sawaguchi T, Niikuni S, Ikemura T. *Macromolecules* 1982;15:1460–4.
- [22] Bracco P, Brunella V, Luda MP, Zanetti M, Costa L. *Polymer* 2005;46:10648–57.
- [23] Men Y, Rieger J, Strobl G. *Physical Review Letters* 2003;91(9):0955021–0955024.
- [24] Na B, Lv R, Xu W, Yu P, Wang K, Fu Q. *Journal of Physical Chemistry B* 2007;111:13206–10.
- [25] Pawlak A, Galeski A. *Macromolecules* 2005;38:9688–97.
- [26] Edidin AA, Pruitt L, Jewett CW, Crane DJ, Roberts D, Kurtz SM. *Journal of Arthroplasty* 1999;14(5):616–27.
- [27] Wang A, Stark C, Dumbleton JH. *Journal of Biomedical Materials Research* 1995;29:619–26.
- [28] Oral E, Malhi A, Muratoglu O. *Biomaterials* 2006;27:917–25.